Role of Chain Interpenetration in the Adhesion between Immiscible Polymer Melts

Regis Schach,[†,§] Yvette Tran,[†] Alain Menelle,[‡] and Costantino Creton*[,†]

Laboratoire de Physico-chimie des Polymères et Milieux Dispersés, Unité Mixte CNRS−UPMC-ESPCI, 10 Rue Vauquelin, 75231 Paris Cédex 05, France, and Laboratoire Léon Brillouin, CEA-Saclay, Saclay, France

Received April 4, 2007; Revised Manuscript Received June 15, 2007

ABSTRACT: The interfacial thickness and mechanical strength of several model interfaces between immiscible polymer melts were investigated. The interfacial width at equilibrium was determined by neutron reflectivity, and the adhesion energy was determined with an asymmetric probe test method inspired of the tests used for soft adhesives. A very good correlation was found between the adhesion energy and the measured interfacial width in a qualitatively similar way as what was observed for interfaces between glassy polymers. For polymer pairs with χ values ranging from 0.002 to 0.05, the mechanical strength of the interface was controlled by the degree of interpenetration, or in other terms, by the interfacial free energy between the two polymers. For lower values of χ, the interfacial strength was comparable to the fracture strength of the weakest of the two bulk polymers, while for higher values of χ, the thermodynamic work of adhesion and the polymer surface mobility are probably controlling the interfacial strength.

1. Introduction

The role of mutual interpenetration of polymer chains on the mechanical properties of interfaces is well-known and has been the focus of many publications.[1−8] However, most of these publications have considered adhesion between glassy polymers where the interface was formed at high-temperature (above the glass transition temperature of the polymers) and was mechanically tested at room temperature (below the glass transition temperature of the polymers). In that situation, the formation of the interface is controlled by kinetics if the two polymers are miscible or by thermodynamics if the two polymers are immiscible. In both cases the mechanical strength of the interface depends on the plasticity mechanisms of the polymers in the glassy state.[8]

The situation is markedly different for adhesion between polymer melts, since in this case both the interface formation and the mechanical testing occur above the glass transition temperature of the polymers. This situation is relevant in processing situations where a stress is applied to an interface during the manufacturing process. A classical example of that situation which motivated this study is the manufacturing of rubber tyres where uncured rubber layers of different types are assembled before the final cross-linking takes place.

Hence it is not surprising that most studies on adhesion between polymer melts found in the literature focus on filled un-cross-linked elastomers and have been carried out by rubber specialists.[9−12] This situation is much more complex since the polymer can be strongly bound to the carbon black filler and its mobility (both in the bulk and at the interface) will be much more complex than that of a simple linear polymer chain. Although all studies report increasing adhesion strength with contact time, they did not measure interfacial width or characterize interfaces between immiscible polymers.

From a different community, there is an abundant literature on the adhesion between an elastomer and a miscible polymer brush which has been recently reviewed[13] or between an elastomer and a solid surface with variable chemical composition.[14−17] In these various situations it was shown that if a miscible polymer brush penetrates a cross-linked elastomer, the adhesion is reinforced, and that, in the situation where interpenetration is impossible, the thermodynamic work of adhesion and the surface mobility of the molecules are important parameters controlling the mechanical strength of the interface.

In the present paper, we report new data on the characterization of the interfacial width and on the mechanical strength of a series of interfaces between two polymer melts: one model polymer, *cis*-1,4 polybutadiene, and a series of polymers of similar molecular weight but different chemical structures. All polymers used in this study have glass transition temperatures well below room temperature and the different values of the Flory χ parameter for these polymer pairs result in different depths of interpenetration.

Experimentally, we followed the same strategy as that followed by Schnell et al. for glassy polymers.[6,7] We characterized the interfacial widths of the different polymer pairs by neutron reflectivity and evaluated the mechanical strength of the same interfaces with a fracture test.

A notable difference lies however in the type of mechanical test used to evaluate the mechanical strength. While, for glassy polymers, a classical fracture mechanics test such as the asymmetric double cantilever beam test (ADCB) is well suited[8] to obtain a quantitative value of G_c, this test is not adapted to highly viscoelastic polymer melts. We had therefore to develop a specific mechanical test for our interfaces, inspired by the tests used to characterize the adhesive properties of soft adhesives.[18,19]

2. Theoretical Background

2.1. Polymer Interfaces. The thermodynamics and kinetics of polymer interfaces has been extensively studied both theoreti-

* To whom correspondence should be addressed. E-mail: costantino.creton@espci.fr.

† Laboratoire de Physico-chimie des Polymères et Milieux Dispersés, Unité Mixte CNRS−UPMC-ESPCI.

‡ Laboratoire Léon Brillouin, CEA-Saclay.

§ Current address: Centre Technique de Ladoux, Michelin, Clermont-Ferrand, France.

10.1021/ma0707990 CCC: $37.00
Published on Web 07/27/2007

cally and experimentally.[20−24] If the two polymers on both sides of the interface have a nonzero χ parameter, the interfacial width will be finite and at thermodynamic equilibrium, will be given by[21]

$$w = w(N=\infty)\frac{1}{\sqrt{1-2\ln 2\left(\frac{1}{\chi N_A}+\frac{1}{\chi N_B}\right)}} \quad (1)$$

where

$$w(N=\infty)=\frac{a}{\sqrt{c\chi}} \quad (2)$$

and a is the segment length and c is a constant which has a value of 6 or 9 depending on whether the interface is in the weak or strong segregation limit.

2.2. Determination of Interfacial Width and Interpenetration Depth with Neutron Reflectivity. The width of the polymer−polymer interfaces is usually measured by neutron reflectivity which is an ideal technique to measure interfacial widths[24] ranging between 2 and 30 nm with a resolution of the order of magnitude of several angstroms. This technique is sensitive to gradients of the scattering length density, which depends directly on the composition of the layers. Because of the big difference in scattering length densities between hydrogen and deuterium, it is possible to obtain a very good contrast between two polymers using isotopic substitution of hydrogen by deuterium.

Since there is no direct inversion method of the data, the reflectivity profiles as a function of wave vector k can be fitted with a variety of functions depending on what the deuterium and hydrogen concentration profile is expected to be. The experimental data were all fitted using a model of two layers of constant scattering length density, adjustable thickness and interfacial width. The two polymer layers are connected with the following error function:

$$\mathrm{erf}\left(\frac{(z-z_0)}{\sigma}\right)=\frac{2}{\sqrt{\pi}}\int_0^{(z-z_{0i})/\sigma} e^{-t^2}\,dt \quad (3)$$

where z_0 is the position of the interface between the two polymer layers and 2σ is defined here as its full width.

To measure the interpenetration width from the raw data, the contribution to the interfacial width of the capillary waves[25] needs to be evaluated. Following Jones and Richards,[25] and using eq 1 and 2, this contribution can be written as

$$\langle \Delta z^2 \rangle \approx \frac{3w}{\pi\rho a^2}\ln\left(\frac{l}{w}\right) \quad (4)$$

with w the interpenetration width, l the coherence length of the neutron beam (order of magnitude of 20 μm), ρ the density, and a the Kuhn length. As the capillary wave contribution is a function of the interpenetration between the two polymers, it cannot directly be calculated from the experimental results but needs to be determined by successive iterations until the calculation converges toward the real $<\Delta z^2>$ and w values.

2.3. Mechanical Strength of Polymer Interfaces. The situation concerning the mechanical strength is on the other hand much less understood. For polymer glasses forming crazes, Brown's model of polymer toughness[26] provides a molecular interpretation of the crack tip dissipation and links the molecular structure of the interface (degree of interpenetration) with its toughness. This model implies, however, the existence of a clear yield stress for the polymer which does not exist for polymer melts.

Furthermore, polymer melts do not localize stresses at a crack tip like polymer glasses but tend to deform much more homogeneously effectively removing sharp stress concentrations. Only two techniques have been used to investigate the mechanical and adhesive properties of polymer melts, peel tests[9,27] and contact mechanics tests using probes.[12] In both cases, the polymer melt is in the form of a film and the result coming out of the test is not based on the release of elastic energy but rather on a reasonable evaluation of the external work provided by the operator to break the sample or the interface.

Because we were interested in varying contact times in a range of values of the order of seconds to minutes, we used a contact mechanics method inspired from what is used for pressure-sensitive adhesives[28,29] and described in more detail in the Experimental Section. In this method, the two polymer melt surfaces are put in contact for a given time, therefore allowing interdiffusion and/or equilibration of the interfacial structure. They are then separated, at the same temperature, by applying a tensile force. The geometry is that of parallel disks being pulled apart at a constant velocity. The force displacement curve is then recorded, and the energy of separation W_{adh} is measured as the integral of the force displacement curve normalized by the contact area.

In a separate paper,[30] we have studied in detail the fracture mechanisms between two polymer melt layers in this geometry for a range of interfacial widths and molecular weights of the linear polymers. Although we do not want to discuss the details here, the most important result is the existence of three types of failure mechanisms of the interface:

- For average strain rates lower than the inverse of the terminal relaxation time of the polymer, the fracture occurs in the bulk and is not sensitive to the presence of the interface. The situation is very similar to that of the fracture of a homogeneous polymeric fluid which has been extensively studied for poly(dimethylsiloxane fluids).[31−33]
- For average strain rates higher than the inverse of the terminal relaxation time of the polymer, two mechanisms are observed: an interfacial crack propagation mechanism[34,35] for weak interfaces and a bulk deformation[36] of the layer(s) for strong interfaces.

In this paper, we will focus on the second case, i.e., high strain rates, which is the most sensitive to the structure of the interface. Depending on the nature of the polymer pair, we will characterize the adhesion energy at thermodynamic equilibrium and the type of failure mechanism.

3. Experimental Section

3.1. Materials. We used a linear polybutadiene (PB) (M = 420 kg/mol, more than 80% 1,4) with a well-defined micro- and macrostructure as our reference material (PB420K-H). We measured the adhesion properties of several elastomers with this PB: three linear styrene−butadiene random copolymers (SBR) with the same chemical composition (40% styrene) and different molecular weights (80, 160, and 240 kg/mol), one linear SBR with another type of microstructure (36% styrene) and a molecular weight of 160 kg/mol and three "industrial" rubbers with probably some degree of branching: an ethylene−propylene-diene copolymer (EPDM), a polyisobutylene (PIB), and a poly(dimethylsiloxane) (PDMS). For the neutron reflectivity experiments, we measured the interfacial width between each one of these polymers and a deuterated PB with the same chemical structure than PB420K-H but with M = 120 kg/mol (PB120K-H). The relevant characteristics and nomenclature of the materials are summarized in Table 1.

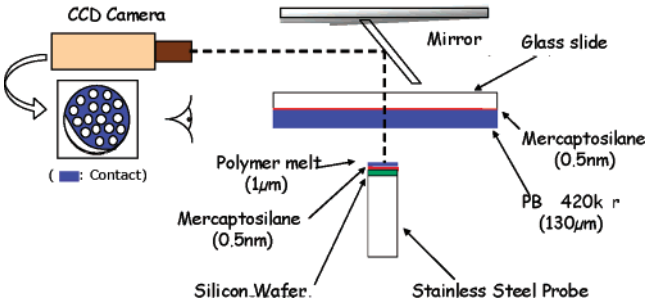

Figure 1. Schematic of the experimental setup for the probe test.

Table 1. Characterizations of the Polymers Used in the Study

	M_n (g/mol)[a]	PDI[a]	% 1,2[b]	% styrene[b]
PB420K-H	420 000	1.1	<20	
PB120K-D	130 300	1.09	<20	
SBR80K	83 000	1.03	11	41
SBR160K	139 800	1.08	11	40
SBR240K	213 100	1.13	12	39
SBR36%Sty	153 100	1.09	8	36
EPDM	115 200	3.18		
PIB	172 000	2.39		
PDMS	1000 000	<2		

[a] By triple detection SEC. [b] By ^{1}H NMR.

3.2. Rheology. The linear viscoelastic properties of the PB420K-H (mechanical reference of our study) were measured in the linear viscoelastic regime on a RDAII parallel plate rheometer from Rheometrics for a range of temperatures. Master curves were then constructed from the tan δ data.

3.3. Probe Test Experiments. We performed probe test experiments on our custom-designed apparatus based on an MTS 810 hydraulic testing machine.[29] Our version of the probe test is based on the contact of a flat punch on a relatively thick soft layer deposited on a hard substrate. The flat punch is a cylindrical stainless steel probe with a silicon wafer glued on its end, the surface of which has been coated with a $\sim$ 1 μm layer of soft polymer. The hard substrate is glass and has been coated with a 130 μm thick reference PB420K-H layer. The experiment itself can be divided into three stages (Figure 1). In the first stage, the cylinder (1 cm in diameter) approaches the glass slide at a constant velocity and comes in contact. When the contact pressure of 1 MPa is reached, the probe stops during a contact time t_c varying from 300 to 2000 s (until thermodynamic equilibrium is achieved at the interface). The probe is then removed from contact during stage 3 at a constant debonding velocity $V_{deb} = 100$ μm/s.

During this test, all experimental parameters are well controlled. The contact pressure, the contact time and the debonding velocity are independent parameters of the test and the contact area is measured with the video acquisition which also allows the detailed analysis of the debonding mechanism. As described elsewhere[19] and shown in Figure 2, the result of the experiment is a force−displacement curve which can then be converted to a stress−strain curve by normalizing the force by the contact area between the probe and the soft layer and by normalizing the displacement by the initial thickness of the layer h_0. The integral under the stress−strain curve multiplied by the thickness of the layer is then defined as the adhesion energy W_{adh}.

To avoid debonding of the two polymer layers from the glass or from the silicon substrate during the test, we used self-assembled monolayers of mercaptosilane to chemically bond the polymer layers to the substrates. First, the substrates (glass slide or silicon wafer) are cleaned in a piranha bath (30% hydrogen peroxide, 70% sulfuric acid at 150 °C) during half an hour. Then, they are put in a solution of 10% 3- mercaptopropyl trimethoxysilane in toluene. The reaction is carried out in inert atmosphere (nitrogen) during 3 h. The substrates are finally rinsed with absolute toluene and dried with a nitrogen flux. For glass slides, a solution of 10% SBR in toluene is poured on the substrates, the toluene is slowly evaporated

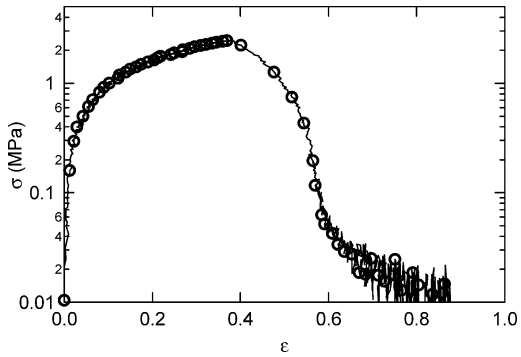

Figure 2. Typical stress−strain curve obtained during the removal of the probe at 100 μm/s after a certain contact time allowing the interdiffusion of polymer chains at the interface.

and the substrates are then annealed at 45 °C during 2 days, to allow the reaction of the SH group with the double bonds of the SBR to take place. This last step yields a 130 μm layer of rubber on the glass substrate. For the silicon wafer, a 1 μm layer of polymer is spin-coated on the substrate, which is then annealed at 45 °C over 2 days, during which the mercapto group can react with the double bonds of the polymer.

As discussed in the Introduction, in order to obtain meaningful comparisons of adhesion energies for the different fluid/fluid interfaces, we always performed the tests at a probe velocity during the debonding stage which imposed average initial strain rates to the samples, higher than the inverse of the longest relaxation time of both polymers. For linear polymers this can be written as

$$V_{deb} > h_0/\tau_d \tag{5}$$

where τ_d is the terminal relaxation time of the polymer melt at the test temperature.

Furthermore, the chemical nature (PB420K-H) and thickness of the thick layer (130 μm) was always kept constant. Under those conditions, the other polymers (the 1 μm thick layer) acted as boundary conditions for the deformation of the PB420K-H layer, but their deformation did not contribute to the adhesion energy. This latter point deserves further discussion. Our experimental concern was to use a layer thick enough to reproduce the chain surface conformations of thick layers, while acting essentially as a brush with minimal viscous dissipation in the thin layer during debonding. We used several thicknesses between 1 and 3 μm, and results were not affected. We also checked that, after the test, the thin layer was of an equivalent thickness or higher as measured by ellipsometry. This condition was clearly met for weak interfaces and was met for strong interfaces (PB/SBR) when the PB was the thick layer.

3.4. Samples for Neutron Reflectivity Measurements. We measured the interfacial width between two immiscible polymers using neutron reflectivity. The preparation of the samples for these experiments is a key aspect of our work. To conduct such measurements, we need to build double layers of polymers with a thickness of several tenths of nanometers, with a very low roughness (of the order of magnitude of 1 Å), on a surface of several square centimeters. There are several methods to build double polymer layers of this size. For example, it is possible to use spin-coating to prepare a thin polymer layer on a silicon substrate. The second layer can be prepared using spin-coating a second time, with a solvent for the second polymer, which is a nonsolvent of the first polymer. Unfortunately, the chemical structures of the polymers of this study are too close, and to our knowledge, they have the same solubility properties.

Another technique can be used to prepare ultrathin double layers of glassy polymers: the floating technique. In this technique, two thin films are prepared by spin-coating on two different substrates. One of the thin films is floated off the substrate onto deionized water surface and is picked up by the second film which was still on its substrate. Unfortunately, it is impossible to use the floating

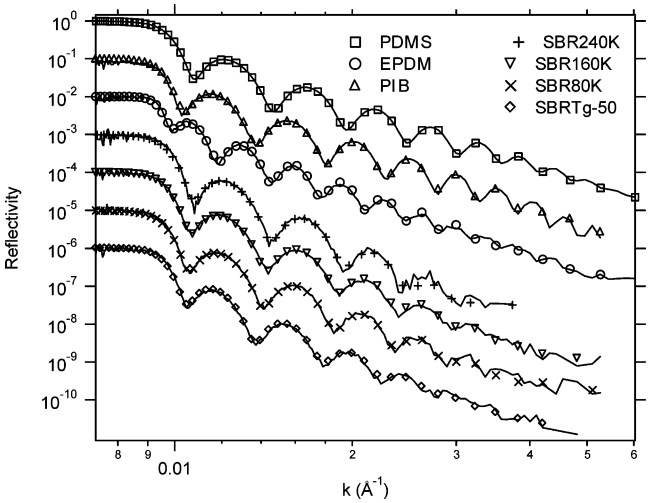

Figure 3. Experimental (symbols) and calculated (lines) reflectivity curves using an error function to describe the interface.

technique with a liquid and hydrophobic material. On water, the liquid film retracts to minimize surface energy, and the excellent surface roughness of the spin-coated film is lost during the process.

To build reflectivity samples with polymeric liquids, we used a combination of both techniques. A first layer of polymer is spin-coated on a silicon wafer grafted with the self-assembled monolayer of mercaptosilane. The grafting stabilizes the polymeric layer, since without it, the film dewets for surface energy reasons. Second, a polymethyl methacrylate (PMMA) layer is spin-coated on a glass substrate. On this PMMA layer, a second liquid polymer layer is spin-coated, using a carbon tetrachloride solution (which is a non solvent of PMMA) to yield a double layer PMMA/liquid polymer. The PMMA is a glassy material, so this double layer can be floated onto deionized water and picked up (from the top) by the first layer, to yield a triple layer of two polymeric fluids and PMMA on the first silicon wafer. This sample is then washed with acetone, which is a good solvent of PMMA and a non solvent of the polymeric fluids used in our study. Using this procedure, we can obtain double layers of polymeric fluids with low enough surface roughness to conduct reflectivity experiments. The surface roughness of our samples was measured at different scales between each step using AFM and ellipsometry and is of the order of magnitude of several angstroms.

Neutron reflectivity experiments were performed at room temperature using the EROS reflectometer at the Laboratoire Leon Brillouin (CEA-Saclay). The acquisition was carried out by 30 min intervals during 4 h, and the 8 signals obtained were compared in order to check if the interface was at thermodynamic equilibrium. The reflectivity data were analyzed with the methodology presented in section 2.2. The procedure consists of fixing the values of the scattering length density and finding the thicknesses of the layers and the interface width as parameters for which the calculated reflectivity curve best fits the experimental reflectivity data. We compared systematically the thicknesses of the polymer layers obtained by neutron reflectivity with the values measured by ellipsometry, and we obtained a very good agreement between the two measurements.

4. Results and Discussion

4.1. Determination of the Interfacial Width by Neutron Reflectivity. In our neutron reflectivity experiments, we measured the interfacial width between the deuterated layer made of PB120K-D and the hydrogenated layer made of the other polymeric fluid (SBR, PIB, EPDM, or PDMS).

Figure 3 shows the reflectivity curves obtained at thermodynamic equilibrium for all samples of the study and the best fits obtained with the methodology described in section 2.2.

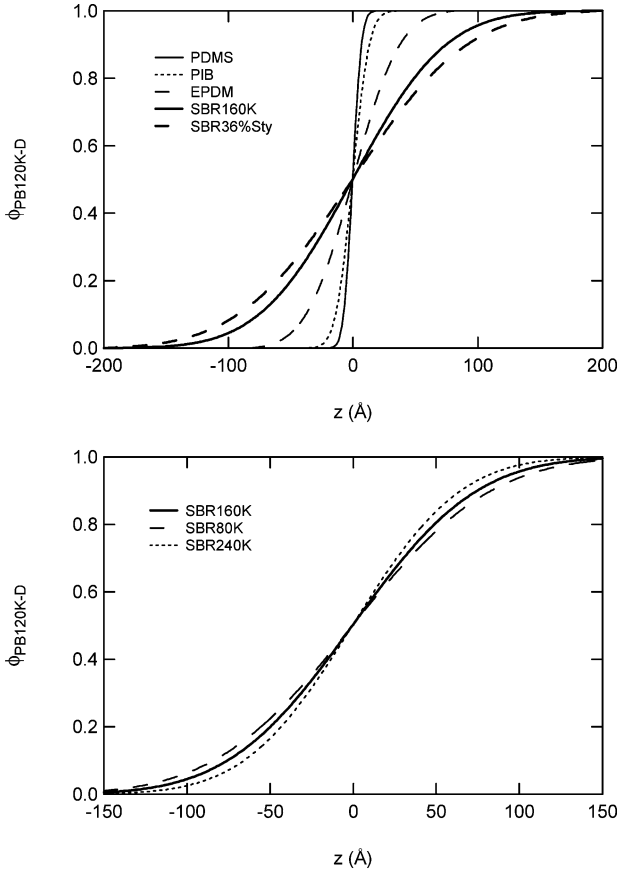

Figure 4. Volume fraction of deuterated monomer as a function of distance along the interface for interfaces between a deuterated PB and various polymers: (a) various polymers with different monomer composition; (b) three SBR polymers with identical monomer composition but different molecular weights.

Table 2. Relevant Characteristics of the Polymer−Polymer Interfaces[a]

	2σ (Å)	w (Å)	Flory parameter χ	Kuhn length at interface (Å)
SBR36%Sty	228 ± 5	204 ± 6	0.0023 ± 0.0006	9 ± 2
SBR160K	207 ± 10	184 ± 10	0.0033 ± 0.0009	9 ± 2
SBR240K	188 ± 5	165 ± 6	0.0033 ± 0.0009	9 ± 2
SBR80K	165 ± 10	144 ± 10	0.0033 ± 0.0009	9 ± 2
EPDM	100 ± 5	82 ± 6	0.006 ± 0.002	7 ± 3
PIB	42 ± 5	30 ± 7	0.04 ± 0.02	7 ± 3
PDMS	26 ± 4	16 ± 5	0.15 ± 0.05	7 ± 3

[a] The deuterated polymer is always PB-120K-D.

The agreement between the experimental data (symbol) and the simulation (solid line) is in general very good.

Figure 4 shows the volume fraction profiles of the deuterated polymer PB120K-D corresponding to the best fit of the neutron reflectivity data. The captions indicate the various hydrogenated elastomer layers studied. Figure 4a shows the effect of changing the monomer composition while Figure 4b illustrates the effect of changing the molecular weight at identical monomer composition. From these data characterizing the interfacial width, the interpenetration distance of the polymer chains can be calculated by subtracting the broadening due to capillary waves, and the final results are summarized in Table 2.

The expected variations of interfacial width with molecular weight are observed for the three SBR polymers with the same chemical structure (Figure 5b): the higher the molecular weight, the sharper the interface. This gives us a simple way to estimate the Kuhn segment length. Equation 1 for the interfacial width

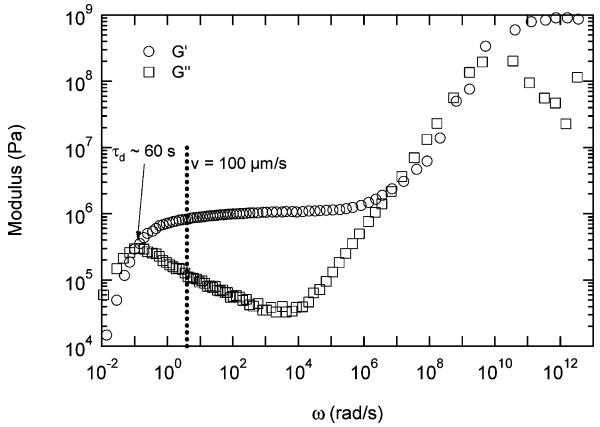

Figure 5. Master curves of the PB420K-H used for the adhesion experiments.

can be rewritten to give the following expression for χ (for a wide interface, with $c = 9$):

$$\chi = \frac{a^2}{9w^2} + 2\ln 2\left(\frac{1}{N_A} + \frac{1}{N_B}\right) \quad (6)$$

Using eq 6, we can calculate both the Kuhn length at the interface and the Flory interaction parameter for the 3 SBR's with the same chemical structure. This method gives a Kuhn length of 9 Å, significantly higher than the Kuhn length in the bulk polymer which is expected to be of the order of magnitude of 5 Å. Schnell and co-workers[6] reported a similar result on a PS/PpMS interface: the Kuhn length estimated from NR data appears to be approximately twice the bulk value.

We used this value of the Kuhn length to calculate the Flory parameter for the SBR36%sty/PB120K-D interface. These systems have very similar structures and there is no reason for a very different Kuhn length value.

For the other three elastomers, we considered a Kuhn length of the same order of magnitude, between 5 and 10 Å. We used eq 2 for infinite molecular weight with $c = 6$ (sharp interface) to calculate the χ value of these polymers. The results of this calculation are less accurate than the calculations for the SBR, because of this lack of experimental data.

Table 2 summarizes the relevant characteristics of the interfaces studied here. The sharpest interface is the PDMS/PB interface, with an interpenetration width w of 16 Å and a Flory parameter very high of 0.15. The PIB forms a wider interface with PB (with $w = 30$ Å) giving a monomer−monomer interaction parameter of 0.04. The order of magnitude of the EPDM interface (82 Å) is closer to the radius of gyration of the polymers (order of magnitude of 150 Å), with a χ of 0.006. SBR rubbers have the widest interfaces, with interpenetrations between 150 Å and 200 Å. The χ parameter for the three SBR40% polymers with PB is 0.0033, 2 orders of magnitude less than the PDMS/PB. Finally, the SBR with a lower styrene content has the widest interface with 204 Å and a Flory parameter with PB of 0.0023. This result is consistent with the fact that the immiscibility between PB and SBR comes from the styrene part of the SBR.

4.2. Linear Viscoelastic Properties. To obtain meaningful measurements of the adhesion energy, we have to test the materials at an average deformation rate that lies in the elastic domain (to avoid a fluid fracture in the bulk), so that the value of the reptation time sets the minimum debonding velocity for the probe test experiments as described in section 2.3.

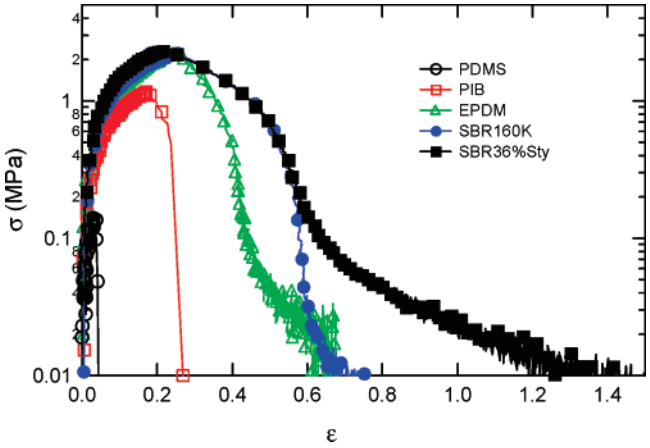

Figure 6. Stress−strain curves obtained with the probe test at room temperature and $V_{deb} = 100$ µm/s for the interfaces between PB420K-H and polymers with: different monomer compositions.

From the frequency sweeps at different temperatures, master curves shown in Figure 5 could be constructed using the time−temperature equivalence principle. For monodisperse linear polymers, several molecular and dynamic parameters of the polymer can be extracted from the master curves, and in particular the reptation time at room temperature which determines the limiting strain rate below which the polymer melt behaves as a fluid. We measured for the PB420K-H a reptation time of 60 s, so we used a debonding velocity of 100 µm/s. For a layer thickness of 130 µm, this probe velocity imposes a nominal initial strain rate of 0.7 s^{-1}, more than a decade higher than the threshold value for liquid behavior determined approximately by the inverse of the reptation time.

4.3. Determination of the Adhesion Energy. We used the probe tester apparatus described in the experimental section to measure the adhesion energy for all the interfaces at thermodynamic equilibrium and also the fracture energy of pure PB420K-H in contact with itself. To be certain that we have reached the thermodynamic equilibrium, we tested the same interface with increasing contact times: when the equilibrium is reached, the tack curves become independent of contact time. Equilibrium contact time values varied between 300 and 2000 s depending on the polymer−polymer system.

Figure 6 shows the nominal tensile stress−strain curves obtained for the adhesion measurement at thermodynamic equilibrium for a series of different interfaces. As discussed in the introduction, for a probe debonding velocity of 100 µm/s, the thick PB layer behaves like a viscoelastic solid and two types of debonding mechanisms can be observed: interfacial crack propagation (leading to a very sharp decrease in stress after the maximum) and bulk cavitation (which leads to a more progressive decrease in stress).

The adhesion energy of PDMS on PB is really low, less than 1 J/m^2. The PIB has a better adhesion (22 J/m^2), but the fracture remains brittle and apparently completely interfacial as determined by video observation, with very little bulk deformation of the PB layer (maximum strain of 0.2). The fracture of the EPDM/PB interface is less brittle and the PB layer is completely detached from the EPDM surface for a strain of about 60% with a beginning of bulk fracture and an adhesion energy of 77 J/m^2. Finally, the four SBR/PB systems are characterized by a bulk fracture behavior: fracture occurred in the PB layer, and not at the interface. The adhesion energy measured is very close to the fracture energy of the PB, 120 J/m^2. Note that the high molecular weight SBR and the SBR36%Sty curves show a pronounced tail in the deformation curve. Although it is tempting

to attribute this difference to the interface, one should remember that it is the PB420K-H which deforms in these experiments and the difference is much more likely due to a slight difference in the temperature at which the test was carried out and should not be interpreted further.

We used two different polymers for neutron reflectivity experiments and adhesion energy measurements. Nevertheless, the chemical structure of the two PB was exactly the same, the only difference being the molecular weight. Knowing the molecular weights of all polymers and assuming that χ is independent of molecular weight, we can use the neutron reflectivity results on the PB120K-D to calculate the theoretical interfacial width of the different polymers with the PB420K-H using eq 1. The measured adhesion energy can then be represented as a function of the calculated interpenetration distance.

This comparison is shown in Figure 7 and clearly demonstrates that the adhesion energy between the fluid layers depends strongly on the degree of interpenetration at the interface. Adhesion energy increases from a value of several J/m^2 for a very sharp interface (10 or 20 Å) to the PB fracture energy for interfaces larger than 150 Å. It is important to note for the significance of the comparison that all samples except PDMS were tested in these experiments at a strain rate, which corresponds to their rubbery plateau, as it is the case for PB (Figure 5).

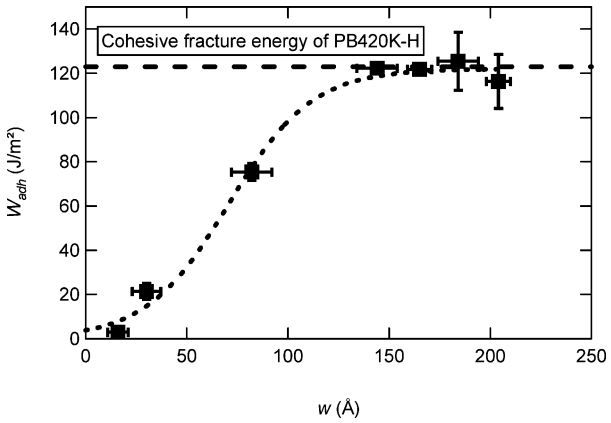

Figure 7. Adhesion energy W_{adh} of interfaces between PB420K-H and different polymers as a function of the interpenetration width at the interface w.

5. Discussion

It is worthwhile to discuss these results in light of the state of the art on adhesion at polymer−polymer interfaces. It has been known for quite some time that for fully miscible identical polymers, mutual interdiffusion at the interface would lead to a higher mechanical strength.[1−8]

However it is only recently that the combination of neutron reflectivity and fracture toughness showed that for glassy polymer pairs, the interpenetration distance needs to be of the order of one entanglement length.[7,37−39] On the other hand the effect of forming entanglements by mutual interdiffusion on mechanical strength of the interface between polymers *above* their glass transition has only been discussed theoretically[2,40] but not studied experimentally to our knowledge, and the required degree of interpenetration is not known.

Yet an analogous situation has been studied more extensively: the adhesion between an elastomer and a solid surface. In this case, one of the polymers is clearly above its glass transition temperature, and if the solid surface is also a polymer, it could be above or below its T_g. Classic studies[14,41−43] for soft polymers on solid surfaces emphasized the role of surface energetics and wrote the thermodynamic (reversible) work of adhesion as

$$W_{rev} = \gamma_1 + \gamma_2 - \gamma_{12} \tag{7}$$

The measured work of adhesion could then be written as[43]

$$G_c = W_{rev}(1 + \phi(a_T v)) \tag{8}$$

where G_c is the critical energy release rate and $\phi(a_T v)$ is a multiplicative factor depending on the dissipative properties of the soft polymer. This classical result obtained for elastomers was later on modified by two important concepts: the role played by the interpenetration of polymer brushes and the possible existence of interfacial slippage. If the solid surface is functionalized with a layer of end-tethered chains fully miscible with the soft polymer, the extraction of the chain from the polymer during debonding contributes significantly both to the measured G_c and also to the dissipative component $\phi(a_T v)$, which is however still represented as a multiplicative factor.[44,45]

Interfacial slippage is important because the surface acts as a boundary condition and if the surface is unable to sustain shear forces, the dissipative shear deformation in the polymer layer during debonding is greatly diminished, reducing the multiplicative factor $\phi(a_T v)$ for the same values of W_{rev} and the same rheological properties of the polymer. The groups of Chaudhury and Leger in particular, showed that resistance to interfacial slippage could be more important than surface energetics and dominate the macroscopic adhesive behavior[16,46−49] and therefore G_c.

For very soft elastomers or polymer melts, however the measurement of G_c as a purely interfacial property becomes difficult since failure does not occur by crack propagation but by a much more complex deformation pattern involving fingering instabilities and the formation of fibrils[19] which cannot be easily separated from the experimental geometry. In this regime the best way to compare adhesive strength of different interfaces is therefore to measure the total work of detachment in the same experimental geometry and this is the parameter defined here as W_{adh}. For these very soft polymers, very few studies exist and either focus on surface thermodynamics changes[18,50] or show only qualitative results.[51]

In the current study, the interpenetration of polymer chains at the interface acts by modifying the boundary condition at the interface: the deeper the interpenetration is and the higher are the interfacial stresses which can be sustained by the interface.

This result has some interesting implications. For high molecular weight polymers in the strong segregation limit, the interfacial width between two polymers 1 and 2 varies as $1/\gamma_{12}$, so from the results of Figure 7, one expects G_c to vary approximately as the inverse of the interfacial tension.[25] This result is directly at odds with eq 7. Since typically the surface tensions are much larger than the interfacial tension, eq 7 would predict a high adhesion between two very immiscible but high surface tension polymeric fluids and on the contrary a low adhesion between two nearly miscible but low surface tension fluids. The point that interpenetration favors adhesion is hardly new. However we show that for interfaces between immiscible polymers, it is best to think in terms of transition from a W_{rev} dominated regime (for high values of χ) to a γ_{12} dominated regime (for low values of χ).

For our weaker interfaces failing by interfacial crack propagation, $W_{adh} \sim G_c$ and we can use fracture mechanics concepts to

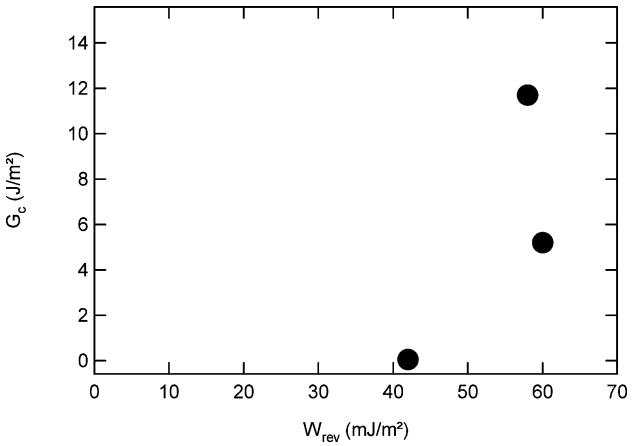

Figure 8. G_c estimated from the probe test curves and eq 9 vs W_{rev}.

illustrate this point more accurately. Webber and co-workers[34] proposed a model to describe the failure of a joint between a confined elastic material and a rigid substrate, in the case of an interfacial failure at relatively low strains. This model, well adapted to describe our experimental adhesion measurements, gives a relationship between the critical energy release rate G_c (characteristic of the resistance to interfacial crack propagation) and the failure average strain ϵ^* (easily measured on the tack curves):

$$\epsilon^* = \left(\frac{G_c}{Eh}\right)^{1/2} \tag{9}$$

with E being the Young modulus of the confined material and h the thickness of the confined layer. We can use this model to estimate G_c for three of our samples: PDMS, PIB, and EPDM, which show an interfacial failure mechanism.

If we use eq 7 and the fact that the interfacial tension $\gamma_{1,2}$ is directly related to the interface width

$$\gamma_{1,2} = kT\rho a\sqrt{\frac{\chi}{6}} = \frac{kT\rho a^2}{6w} \tag{10}$$

we can estimate W_{rev} using our neutron reflectivity measurement to calculate the interfacial tension of the polymer−polymer interfaces and data of the literature for the surface energy of the polymers. Figure 8 shows the calculated G_c value vs the thermodynamic work of adhesion W_{rev}. There is no obvious direct correlation between the thermodynamic work of adhesion and the measured G_c.

A second point, which is interesting to discuss, is the extent of interpenetration which is necessary to obtain a high mechanical strength. The fracture toughness between glassy polymers increases with interpenetration until it reaches the bulk fracture energy for an interpenetration value which varies with the experimental system from 0.5 to 1.5 times the average distance between entanglements d_e in the bulk polymers.[8,37]

Our results show that, for polymer melts, the increase in adhesion energy with interpenetration is more progressive and the maximum adhesion energy is achieved for a deeper interpenetration than d_e: the order of magnitude of the entanglement spacing is 20 Å for the PB and 30 Å for the others polymers and the maximum value is achieved for an interpenetration of 150 Å equivalent to four to five entanglement lengths and comparable to the radius of gyration of the polymers.

These results are also consistent with the theoretically proposed argument[2,40] that, for polymer melts, the adhesion energy should reach its saturation value when the interpenetration distance becomes of the order of the radius of gyration of the polymers and the degree of entanglement at the interface is the same as that in the bulk. This prediction follows from the fact that the force to extract a polymer chain in the melt should increase continuously with molecular weight since entanglements play a lesser role in transferring stress than in the glassy state.

For very high molecular weight polymers and/or temperatures close to T_g, chain fracture rather than chain extraction may occur and modify this result, defining then a critical interpenetration distance for optimum toughness, lower than the radius of gyration of the chains. The situation would then become closer to that of polymer glasses.

To fully reconcile our result with previous results, we need to discuss polymer mobility and tube diameter. In our analysis, we have fully ignored the effect of the monomer friction coefficient in the polymer chain extraction that is very likely to occur at the interface during the failure process and the differences in tube diameter due to different average distance between entanglements on each side of the interface. In polymer glasses, a static friction coefficient for the extraction of an individual polymer chain from an environment of identical polymers can be defined and appears to be very dependent on the monomer composition of the polymer.[37,52] Experiments show that this monomer friction coefficient is static since it represents a threshold force above which extraction of the chain can occur rapidly and catastrophically.

In polymer melts, on the other hand, a dynamic monomer friction coefficient ζ, is well-defined from rheological measurements and is representative of molecular friction.[53] The monomer friction coefficient of a given polymer varies with temperature and at a fixed temperature, is mostly controlled by $T - T_g$. For our different polymers, the T_g values are rather similar to the notable exceptions of PDMS and PIB. Among these two, PIB has an abnormally high friction coefficient[53] which partly compensates for its lower T_g and PDMS is indeed much more mobile. Therefore, it is likely that the very low value of G_c measured for the PB/PDMS interface is due to a combined effect of high mobility and low interpenetration. However for the other polymer pairs the friction coefficient of the polymers should be comparable. Of course the PB polymer will have a much lower value of ζ at room temperature because of its low T_g. The fact that we never obtain higher values of G_c than the bulk polymer interpenetration suggests that the dominant friction coefficient in the extraction process is that of the PB. In other words the maximum stress sustainable by the interface is controlled by the stress to extract PB chains from a more "viscous" matrix.

The effect of different tube diameters is much more difficult to assess and will be the focus of a forthcoming paper on kinetics of strength buildup.[54] However differences in tube diameters make it very difficult to normalize data between different systems. Although ref 54 is qualitatively informative, it should be taken with caution since the value of d_e at interfaces between polymers with different melt tube diameters is not precisely known.

As a concluding remark, it is worthwhile to mention that we studied here the simplest case of linear polymer melts. In practice, the same questions of interpenetration and mechanical strength will exist for branched or partially cross-linked systems and for filled systems, and our experimental approach should equally well be applicable to these systems and will be the object of future investigations.

6. Conclusion

We have developed an original method to measure interfacial strength of polymer melts, in the regime where the structure of the interface is different from that of the melt. This method adapted from the probe test methods used for pressure-sensitive-adhesives uses an asymmetric geometry (one thin and one thick layer) and has the advantage to clearly confine the dissipation to one layer. It can then be used to compare different interfaces and the thick layer simply acts as a viscoelastic probe of the interfacial strength. The same tools used to interpret force−displacement curves of soft adhesives and polymer melts, can then be used for these interfaces. The combination of adhesion energy values and neutron reflectivity measurements of interfacial width provides then a detailed picture of the effect of polymer chain interpenetration on mechanical strength.

We have shown conclusively that for interfaces between immiscible polymer melts, the most important factor controlling the mechanical strength is the degree of interpenetration at the interface. This result can be connected with theories based on wetting where surface energies of the two polymers determine chiefly the work of adhesion. Whenever the Flory χ parameter between two polymers is below 0.05, the mechanical strength of the interface between the polymers in the molten state will roughly increase with $\chi^{-1/2}$ until the interpenetration width reaches a value of the order of the radius of gyration of the polymers. This result should be a clear guideline for processing applications where interfaces between polymer melts are under stress.

The second important result of our study relates to the mechanical strength one can expect from entanglements in the melt. This point has been the focus of recent research since it is important for many processing applications. We have shown that the level of interpenetration necessary to retrieve the bulk strength of the interface between two polymer melts is of the order of several entanglements rather than one entanglement as in polymer glasses. This result is not unexpected since chains can be extracted much more easily from polymer above their glass transition temperature than from glasses, but it is the first time that it is conclusively and quantitatively shown.

Acknowledgment. We are grateful to the Manufacture de Pneumatiques Michelin for its financial support and we thank Jean-Michel Favrot and Benoit Salvant at the Ladoux Michelin Technical Center for their continued scientific collaboration in this project. We also are grateful to Fabrice Cousin for help with the neutron reflectivity experiments.

References and Notes

(1) Wool, R. P.; Yuan, B. L.; McGarel, O. J. *Polym. Eng. Sci.* **1989**, *29*, 1340−1367.
(2) Wool, R. P. *Polymer Interfaces*, 1st ed.; Hanser Verlag: Munich, Germany, 1995.
(3) Jud, K.; Kausch, H. H.; Williams, J. G. *J. Mater. Sci.* **1981**, *16*, 204−210.
(4) Prager, S.; Tirrell, M. *J. Chem. Phys.* **1981**, *75*, 5194−5198.
(5) Kausch, H. H.; Tirrell, M. *Ann. Rev. Mater. Sci.* **1989**, *19*, 341−377.
(6) Schnell, R.; Stamm, M.; Creton, C. *Macromolecules* **1998**, *31*, 2284−2292.
(7) Schnell, R.; Stamm, M.; Creton, C. *Macromolecules* **1999**, *32*, 3420−3425.
(8) Creton, C.; Kramer, E. J.; Brown, H. R.; Hui, C. Y. *Adv. Polym. Sci.* **2002**, *156*, 53−136.
(9) Hamed, G. R. *Rubber Chem. Technol.* **1981**, *54*, 576−595.
(10) Hamed, G. R.; Shieh, C. H. *Rubber Chem. Technol.* **1986**, *59*, 883−895.
(11) Ellul, M. D.; Gent, A. N. *J. Polym. Sci., Polym. Phys. Ed.* **1985**, *23*, 1823−1830.
(12) Gent, A. N.; Kim, H. J. *Rubber Chem. Technol.* **1990**, *63*, 613−623.
(13) Léger, L.; Raphaël, E.; Hervet, H. *Adv. Polym. Sci.* **1999**, *138*, 185−225.
(14) Gent, A. N.; Schultz, J. *J. Adhes.* **1972**, *3*, 281−294.
(15) Andrews, E. H.; Kinloch, A. J. *J. Polym. Sci. C: Polym. Symp.* **1974**, *46*, 1−14.
(16) Zhang Newby, B.-M.; Chaudhury, M. K.; Brown, H. R. *Science* **1995**, *269*, 1407−1409.
(17) Ahn, D.; Shull, K. R. *Langmuir* **1998**, *14*, 3646−3654.
(18) Zosel, A. *Colloid Polym. Sci.* **1985**, *263*, 541−553.
(19) Shull, K. R.; Creton, C. *J. Polym. Sci. B Polym. Phys.* **2004**, *42*, 4023−4043.
(20) Helfand, E.; Tagami, Y. *J. Chem. Phys.* **1971**, *56*, 3592−3601.
(21) Broseta, D.; Fredrickson, G. H.; Helfand, E.; Leibler, L. *Macromolecules* **1990**, *23*, 132−139.
(22) Agrawal, G.; Wool, R. P.; Dozier, W. D.; Felcher, G. P.; Zhou, J.; Pispas, S.; Mays, J. W.; Russell, T. P. *J. Polym. Sci., B: Polym. Phys.* **1996**, *34*, 2919−2940.
(23) Guckenbiehl, B.; Stamm, M.; Springer, T. *Physica B* **1994**, *198*, 127−130.
(24) Stamm, M.; Schubert, D. W. *Ann. Rev. Mater. Sci.* **1995**, *25*, 325−356.
(25) Jones, R. A. L.; Richards, R. W. *Polymers at surfaces and interfaces*, 1st ed.; Cambridge University Press: Cambridge, U.K., 1999.
(26) Brown, H. R. *Macromolecules* **1991**, *24*, 2752−2756.
(27) Hamed, G. R.; Shieh, C. H. *J. Polym. Sci., Polym. Phys. Ed.* **1983**, *21*, 1415−1425.
(28) Zosel, A. *J. Adhes. Sci. Tech.* **1997**, *11*, 1447−1457.
(29) Lakrout, H.; Sergot, P.; Creton, C. *J. Adhes.* **1999**, *69*, 307−359.
(30) Schach, R.; Creton, C. In *J. Rheol.* **2007.**
(31) Poivet, S.; Nallet, F.; Gay, C.; Fabre, P. *Europhys. Lett.* **2003**, *62*, 244−250.
(32) Poivet, S.; Nallet, F.; Gay, C.; Teisseire, J.; Fabre, P. *Eur. Phys. J. E* **2004**, *15*, 97−116.
(33) Derks, D.; Lindner, A.; Creton, C.; Bonn, D. *J. Appl. Phys.* **2003**, *93*, 1557−1566.
(34) Webber, R. E.; Shull, K. R.; Roos, A.; Creton, C. *Phys. Rev. E* **2003**, *68*, 021805.
(35) Josse, G.; Sergot, P.; Dorget, M.; Creton, C. *J. Adhes.* **2004**, *80*, 87−118.
(36) Lakrout, H.; Creton, C.; Ahn, D.; Shull, K. R. *Macromolecules* **2001**, *34*, 7448−7458.
(37) Benkoski, J.-J.; Frederickson, G. H.; Kramer, E. J. *J. Polym. Sci. B Polym. Phys.* **2002**, *40*, 2377−2386.
(38) Benkoski, J.-J.; Frederickson, G. H.; Kramer, E.-J. *J. Polym. Sci. B Polym. Phys.* **2001**, *39*, 2363−2377.
(39) Silvestri, L.; Brown, H. R.; Carra, S. *J. Chem. Phys.* **2003**, *119*, 8140−8149.
(40) Aradian, A.; Raphael, E.; de Gennes, P. G. *Macromolecules* **2002**, *35*, 4036−4043.
(41) Andrews, E. H.; Kinloch, A. J. *Proc. Roy. Soc. London, A* **1973**, *332*, 385−399.
(42) Andrews, E. H.; Kinloch, A. J. *Proc. R. Soc. London, A* **1973**, *332*, 401−414.
(43) Maugis, D.; Barquins, M. *J. Phys. D: Appl. Phys.* **1978**, *11*, 1989−2023.
(44) Creton, C.; Brown, H. R.; Shull, K. R. *Macromolecules* **1994**, *27*, 3174−3183.
(45) Deruelle, M.; Léger, L.; Tirrell, M. *Macromolecules* **1995**, *28*, 7419−7428.
(46) Zhang Newby, B. M.; Chaudhury, M. K. *Langmuir* **1997**, *13*, 1805−1809.
(47) Chaudhury, M.; Zhang Newby, B.-M. *Langmuir* **1998**, *14*, 4865−4872.
(48) Léger, L.; Amouroux, N. *J. Adhes.* **2005**, *81*, 1075−1099.
(49) Amouroux, N.; Petit, J.; Léger, L. *Langmuir* **2001**, *17*, 6510−6517.
(50) Toyama, M.; Ito, T.; Nukatsuka, H.; Ikeda, M. *J. Appl. Polym. Sci.* **1973**, *17*, 3495−3502.
(51) Costa, A. C.; Chiche, A.; Vlcek, P.; Creton, C.; Composto, R. J. *Polymer* **2004**.
(52) Washiyama, J.; Kramer, E. J.; Creton, C.; Hui, C. Y. *Macromolecules* **1994**, *27*, 2019−2024.
(53) Ferry, J. D. *Viscoelastic Properties of Polymers*, 3rd ed.; Wiley: New York, 1980; Vol. 1.
(54) Schach, R.; Creton, C., submitted to *J. Rheology*.

MA0707990